

# ChemComm

Chemical Communications

[www.rsc.org/chemcomm](http://www.rsc.org/chemcomm)



Journal of the Chemical Society

# Chemical Communications

ISSN 1359-7345



**COMMUNICATION**

Sofia I. Pascu, Tony D. James *et al.*

Ditopic boronic acid and imine-based naphthalimide fluorescence sensor for copper(II)

# Ditopic boronic acid and imine-based naphthalimide fluorescence sensor for copper(II)<sup>†</sup>

 Cite this: *Chem. Commun.*, 2014, 50, 11806

 Received 7th May 2014,  
 Accepted 3rd June 2014

DOI: 10.1039/c4cc03453h

[www.rsc.org/chemcomm](http://www.rsc.org/chemcomm)

 Meng Li,<sup>a</sup> Haobo Ge,<sup>a</sup> Rory L. Arrowsmith,<sup>a</sup> Vincenzo Mirabello,<sup>a</sup>  
 Stanley W. Botchway,<sup>b</sup> Weihong Zhu,<sup>c</sup> Sofia I. Pascu<sup>\*ab</sup> and Tony D. James<sup>\*a</sup>

Copper ions are essential for many biological processes. However, high concentrations of copper can be detrimental to the cell or organism. A novel naphthalimide derivative bearing a monoboronic acid group (BNP) was investigated as a Cu<sup>2+</sup> selective fluorescent sensor in living cells. This derivative is one of the rare examples of reversible fluorescent chemosensors for Cu<sup>2+</sup> which uses a boronic acid group for a binding site. Moreover, the adduct BNP–Cu<sup>2+</sup> displays a fluorescence enhancement with fructose. The uptake of this novel compound in HeLa cancer cells was imaged using confocal fluorescence microscopy techniques including two-photon fluorescence lifetime imaging microscopy.

Fluorescent sensors have been widely investigated in both environmental and biological systems due to their simplicity and high detection limit.<sup>1,2</sup> Copper(II), the third most abundant transition metal ions in the human body after iron(III) and zinc(II),<sup>3</sup> plays a crucial role in biological, environmental and chemical systems.<sup>4,5</sup> Both excess and deficiency in Cu(II) may lead to severe diseases, such as Alzheimer's and Wilson's diseases and haematological manifestations.<sup>6–12</sup> The average normal concentration range of blood copper is 100–150 μg dL<sup>-1</sup> (15.7–23.6 μM).<sup>13</sup> Therefore, fluorescence probes for copper ions are extensively sought and employed owing to their high sensitivity and the simplicity of equipment requirements.<sup>14–16</sup>

Boronic acids are known to bind 1,2- and 1,3-diol-containing structures through reversible covalent interactions.<sup>17</sup> Such interactions have been used for the preparation of fluorescent sensors and transporters for carbohydrates.<sup>18–20</sup> While, Yoon and co-workers have also utilized boronic acid-linked fluorescent chemosensors

to detect metal ions.<sup>21,22</sup> However, to the best of our knowledge these are the only two examples of using boronic acid-based fluorescent chemosensors to detect metal ions directly. Therefore, we decided to explore the use of boronic acid based reporters for the detection of Cu(II), since, a simple method using boronic acid derived sensors would be desirable. The synthetic method that we now report is straightforward, easy to scale up and leads to a simple isolation of desired product. Our system is particularly appealing since no chromatography-based separation procedures were involved post-synthesis. We have also demonstrated the applicability of the system for improved cellular imaging.<sup>23</sup>

Herein, we describe a novel naphthalene derivative bearing a monoboronic acid group “turn-off” chemosensor for Cu<sup>2+</sup> ions. In addition to solution based experiments, the detection of copper ions in HeLa cells was investigated. Moreover, the complex BNP–Cu<sup>2+</sup> is easily obtained and displays a fluorescence enhancement with fructose, which can be considered as a fluorescence based INHIBIT logic gate. That is to say fructose inhibits the fluorescence decrease upon the addition of copper ions.

For the synthesis of our naphthalimide–boronic acid BNP, we first prepared the 2-amino-6-(propylamino)-naphthalene derivative following standard procedures.<sup>24</sup> This intermediate was then reacted with 2-formylphenylboronic acid ester in ethanol under reflux for 3 h. Subsequently the mixture was cooled to room temperature, and the precipitate produced was filtered and washed with hexane to give a yellow solid. We also prepared the naphthalene derivative **1** which does not include a boronic acid group and compound **2**, a simple boronic acid without an additional metal binding site, these compounds were used as controls to illustrate the importance of both the boronic acid and imine moiety (Fig. 1).

To obtain insight into BNP, its absorption (Fig. S1<sup>†</sup>) and emission spectra (Fig. 2) upon titration with Cu<sup>2+</sup> were recorded. Compound BNP in methanol shows a strong band in the UV-vis spectrum with a maximum absorbance at 450 nm. Upon increasing the concentration of Cu<sup>2+</sup> (0–300 μM), an absorption enhancement could be observed with a red-shift to 465 nm in the absorption maximum which indicated the formation of an adduct between BNP and Cu<sup>2+</sup>. The fluorescence at 525 nm is simultaneously

<sup>a</sup> Department of Chemistry, University of Bath, Claverton Down, UK.  
 E-mail: t.d.james@bath.ac.uk, s.pascu@bath.ac.uk; Fax: +44 (0)1225 386231;  
 Tel: +44 (0)1225 386627

<sup>b</sup> Central Laser Facility, Rutherford Appleton Laboratory, Research Complex at Harwell, STFC Didcot OX11 0QX, UK

<sup>c</sup> Shanghai Key Laboratory of Functional Materials Chemistry, Key Laboratory for Advanced Materials and Institute of Fine Chemicals, East China University of Science & Technology, Shanghai 200237, P. R. China. E-mail: whzhu@ecust.edu.cn

<sup>†</sup> Electronic supplementary information (ESI) available: Detailed procedures, characterization data, and additional plots. See DOI: 10.1039/c4cc03453h



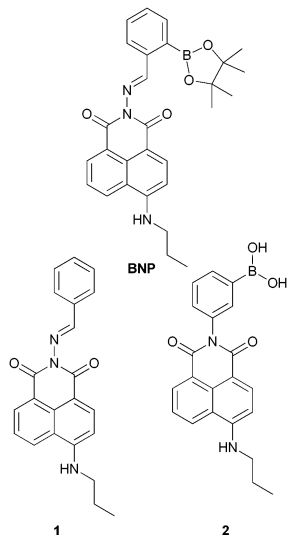


Fig. 1 Structures of boronic acid-conjugated chemosensors (BNP) and control compounds **1**, **2**.

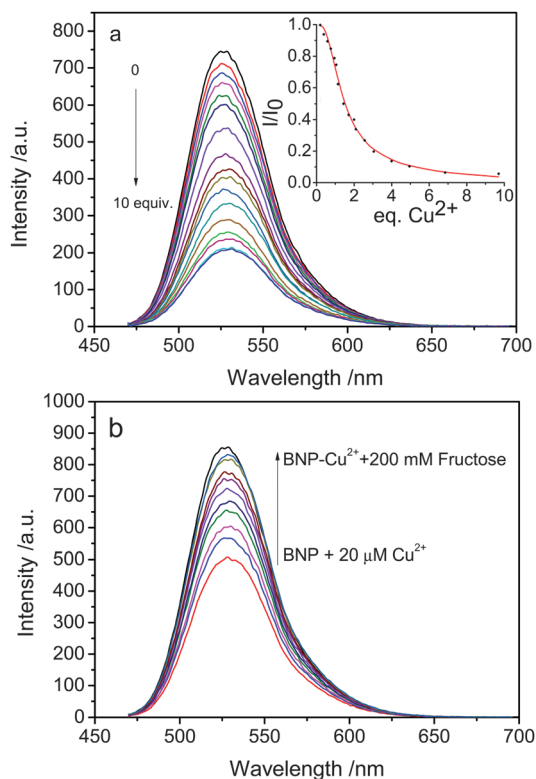


Fig. 2 (a) Fluorescence spectra of BNP ( $1 \times 10^{-5}$  M) in methanol in the presence of different concentrations of  $\text{Cu}^{2+}$  (0–10  $\mu\text{M}$ ) with an excitation at 450 nm. Inset: fluorescence intensity at 525 nm of BNP as a function of  $\text{Cu}^{2+}$  concentration. (b) Fluorescence spectra of BNP- $\text{Cu}^{2+}$  ( $1 \times 10^{-5}$  M) in the presence of different concentrations of fructose when excited at 450 nm.

quenched, which was attributable to the coordination of the paramagnetic  $\text{Cu}^{2+}$  center as reported in previous studies.<sup>21,23</sup> A job plot indicates that the binding of BNP with  $\text{Cu}^{2+}$  has 2 : 1 stoichiometry (Fig. S3<sup>†</sup>). Based upon the results of the fluorescence

titration experiments, the association constant of BNP for  $\text{Cu}^{2+}$  was determined to be  $3.39 \times 10^5 \text{ M}^{-1}$  (Fig. S2<sup>†</sup>). In agreement with the stoichiometry of the reaction the best fitting of the binding model displays a second binding constant which was found to be  $50 \text{ M}^{-1}$ . The discrepancy of the two values indicates the presence of a secondary event in solution which is slower but necessary to complete the “turn-off” process.

In order to further investigate BNP, the fluorescence behavior of BNP toward various metal ions was investigated in methanol (Fig. S4<sup>†</sup>). Metal ions such as  $\text{Na}^+$ ,  $\text{Zn}^{2+}$ ,  $\text{Ag}^+$ ,  $\text{Fe}^{3+}$ ,  $\text{Fe}^{2+}$ ,  $\text{Ni}^{2+}$ ,  $\text{Cd}^{2+}$ ,  $\text{Hg}^{2+}$ , and  $\text{Pb}^{2+}$  show subtle changes, but only the addition of  $\text{Cu}^{2+}$  to BNP gave a significant decrease of fluorescence intensity by 75%.

In order to probe the role played by the boronic acid group in copper ion binding and fluorescence quenching, compound **1** was treated with  $\text{Cu}^{2+}$  in methanol. No changes in the fluorescence properties of **1** were observed, suggesting the importance of the boronic acid moiety in BNP for the binding of copper ions (Fig. S5<sup>†</sup>). As another control, the simple boronic acid derivative **2** without the imine metal recognition site was investigated with  $\text{Cu}^{2+}$  under the same conditions. In this system fluorescence quenching was not observed, which indicates that the imine group plays a role in the coordination of  $\text{Cu}^{2+}$  (Fig. S6<sup>†</sup>).<sup>25</sup> This suggests that the boronic acid and Schiff base work together to bind copper(II) ions in polar environments.

It is well known that boronic acids have high affinities for substances that contain vicinal diol groups. Thus, we decided to use BNP to detect fructose. While BNP did not show any fluorescent changes upon addition of fructose (Fig. S7<sup>†</sup>), the addition fructose to a solution of BNP- $\text{Cu}^{2+}$  resulted in a fluorescence enhancement (Fig. 2). When 2 equivalents of  $\text{Cu}^{2+}$  are added to the BNP solution followed by fructose addition the system behaves like a fluorescence INHIBIT logic gate (Fig. 3).

The capacity of the boronic acid-linked BNP to detect copper ions was investigated in HeLa cells using confocal imaging and fluorescence lifetime imaging (FLIM). Fluorescence lifetime is often considered as a means of distinguishing between different fluorophores, different energy states of the same fluorophore and environmental effects such as quenching caused by binding of intracellular ions such as  $\text{Cl}^-$  or  $\text{Ca}^{2+}$  or oxygen. FLIM was likewise used to monitor the stability and demetallation of metal complexes, including Cu(II), in cancer cells.<sup>26,27</sup> Therefore by utilising an approach of fluorescence lifetime imaging the presence of Cu(II) ions could be investigated by mapping the submicron cellular localisation on ions. Furthermore, a recent study showed that a variant of human apocarbonic anhydrase II could monitor Cu(II) ions in cells *via* FLIM, whereby an increase in Cu(II) ions produced a decline in the average lifetime observed.<sup>28,29</sup> We have combined FLIM and multiphoton excitation in this study to offer reduced effect of the excitation light since the use of near infrared leads to reduced cellular phototoxicity. Further advantages of two-photon excitation is that imaging occurs only from the focal plane, and causes less damage to cells than single-photon microscopy and decreases photo-bleaching, whilst improving imaging depth.<sup>30,31</sup>

Two-photon excitation of the boronic acid-linked BNP, its quenching by  $\text{Cu}^{2+}$  and recovery upon addition of fructose was



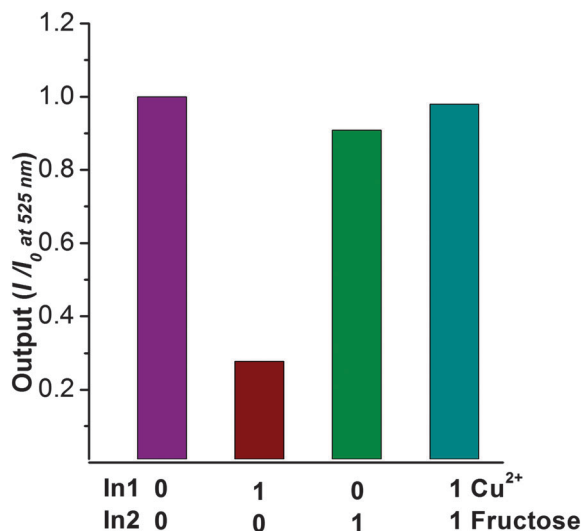


Fig. 3 Column spectra with  $\text{Cu}^{2+}$  (50  $\mu\text{M}$ ) and D-fructose (200 mM) as inputs.

investigated in DMSO solution at 10 mM. DMSO was used due to its low volatility in comparison to methanol and was also employed for the stock solution in the cellular experiments (0.5% DMSO). When BNP was excited at 910 nm, an intense emission was observed, which was quenched after addition of 5 equivalents of  $\text{Cu}^{2+}$ . However, an additional 5 equivalents of fructose led to an enhancement of the fluorescence (Fig. 4). Moreover, the Time-Correlated Single Photon Counting (TCSPC) was measured (Fig. 5). For BNP the first lifetime component ( $\tau_1$ ) was 2.0 ns (25.0%), with a second component ( $\tau_2$ ) of 9.4 ns (75.0%) and a mean lifetime ( $\tau_m$ ) of 7.6 ns. By adding 5 equiv.  $\text{Cu}^{2+}$ , the lifetime of BNP decreased to 4.5 ns. Furthermore, upon addition of fructose, the lifetime component decreased further to 4.1 ns.

Confocal microscopy shows that BNP enters cells and displays strong fluorescence in the absence of external copper ions (Fig. 6 and 7a–c). Furthermore lifetime distribution curve from the FLIM data of BNP showed a  $\tau_1$  of 1.5 ns  $\pm$  0.6 ns, when incubated in HeLa cells, which was comparable to the 2.0 ns  $\tau_1$  observed in solution confirming the presence of the BNP ligand in cells and indicated that the lifetime was not significantly different between DMSO solution and in cells (Fig. 7).

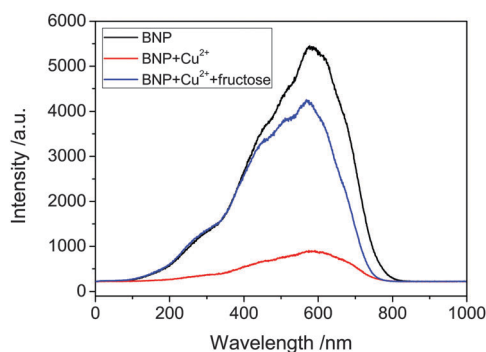


Fig. 4 Emission spectra of BNP (10 mM), BNP plus 5 equiv.  $\text{Cu}^{2+}$  and BNP- $\text{Cu}^{2+}$  plus 5 equiv. fructose with two-photon excitation at 910 nm.

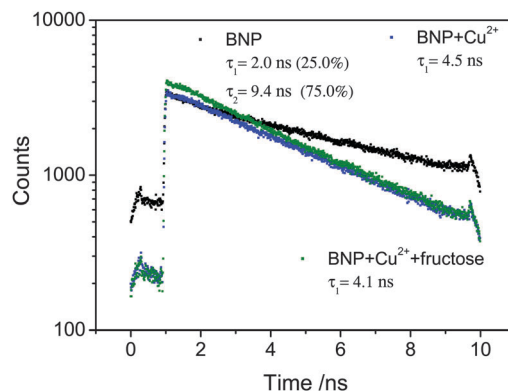


Fig. 5 Nanosecond decay curves for BNP, BNP plus 5 equiv.  $\text{Cu}^{2+}$ , BNP- $\text{Cu}^{2+}$  plus 5 equiv. fructose.

Contrastingly, when 5 equivalents of copper ions (250  $\mu\text{M}$ ) were added a very weak fluorescence response was observed, indicating quenching (Fig. 6 and 7d–f). Moreover, the fluorescence lifetime was observed to have a  $\tau_1$  of 4.4 ns  $\pm$  0.5 ns, which was consistent with data observed in DMSO solution. Further work may shed light upon the interaction of BNP and copper in cells and to fully understand its potential as a copper sensor.

In conclusion, we have developed a robust naphthalimide based fluorescence sensor bearing a monoboronic acid group. The sensor displays high selectivity for copper ions in living cells, which is one of the few examples of boronic acid based fluorescent chemosensors as a copper(II) binding site. With this research we demonstrated that boronic acids can be used to bind metal ions as well as diols. The chelate, BNP- $\text{Cu}^{2+}$ , displayed fluorescence enhancement with fructose, and the system could be described as a fluorescence INHIBIT logic gate. We believe that these results will be of particular interest for the further development of the next generation of molecular ion sensor systems.

T.D.J and M.L. are grateful for financial support from China Scholarship Council (CSC) and University of Bath Full Fees Scholarship.

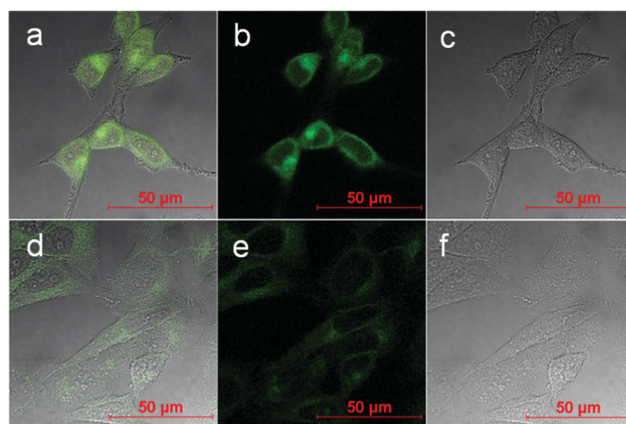


Fig. 6 Laser scanning confocal imaging of BNP in absence of  $\text{Cu}^{2+}$  (a–c), and BNP in presence of  $\text{Cu}^{2+}$  in HeLa cells (d–f). (a) Overlay image of (b) and (c), (d) overlay image of (e) and (f). (b, e) Fluorescence micrographs with excitation at 405 nm and the emission long path filtered at 515 nm, (c, f) differential interference contrast micrograph.



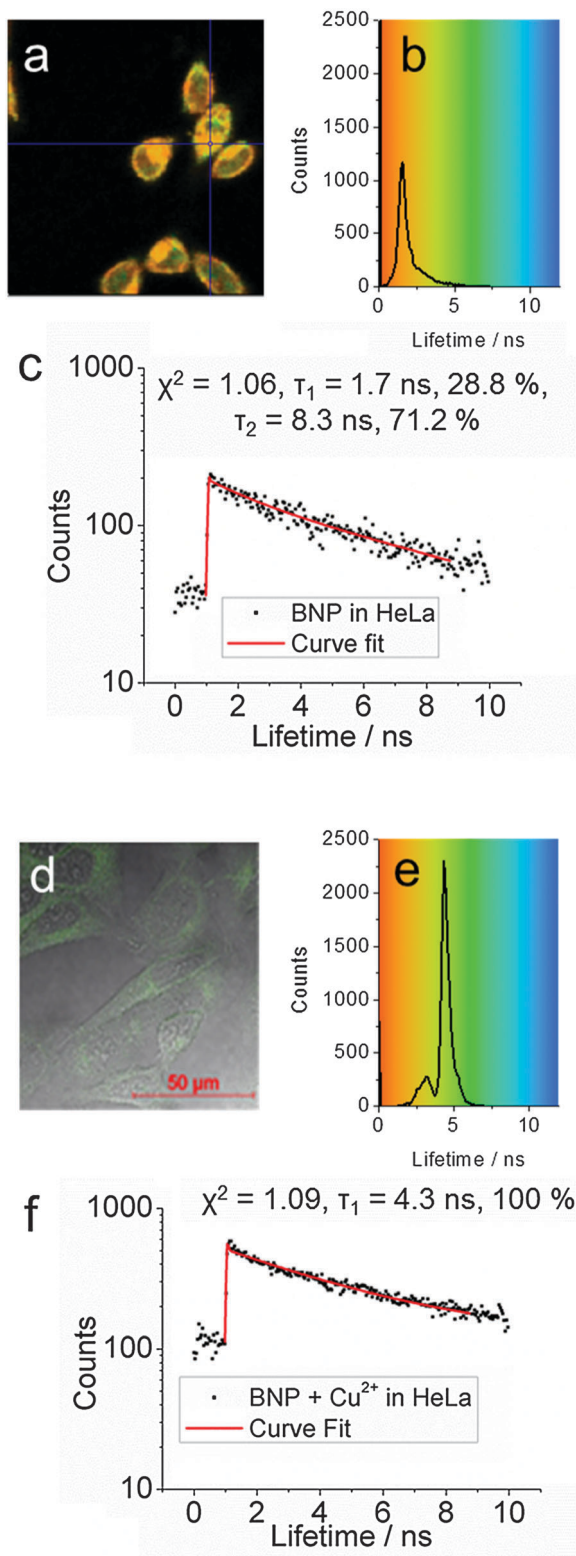


Fig. 7 Two-photon lifetime imaging at 910 nm, 15 min incubation of 50  $\mu\text{M}$  BNP in HeLa cells (0.5% DMSO, 2.5 mW), (a–c) and 50  $\mu\text{M}$  BNP + 250  $\mu\text{M}$   $\text{Cu}^{2+}$ , 5.6 mW (d–f). Images show: (a) fluorescence lifetime mapping for  $\tau_1$  and (d) confocal overlay image of 6e and 6f, (b and e) corresponding fluorescence lifetime distribution curves, (c and f) sample point decay trace inside the cell.

S.I.P. and S.W.B. thank the Royal Society, MRC and STFC for funding. The Catalysis And Sensing for our Environment (CASE) network is thanked for research exchange opportunities. W.H.Z. is grateful for financial support from the Oriental Scholarship, and the Fundamental Research Funds for the Central Universities (WK1013002). T.D.J. thanks ECUST for a guest professorship. T.D.J. also thanks the Royal Society for support.

## Notes and references

- X. Chen, X. Tian, I. Shin and J. Yoon, *Chem. Soc. Rev.*, 2011, **40**, 4783–4804.
- T. Yanagida and Y. Ishii, *Single molecule dynamics in life science*, John Wiley & Sons, 2008.
- A. Sigel, H. Sigel and R. K. Sigel, *Structural and Catalytic Roles of Metal Ions in RNA*, Royal Society of Chemistry, 2011.
- P. Li, X. Duan, Z. Chen, Y. Liu, T. Xie, L. Fang, X. Li, M. Yin and B. Tang, *Chem. Commun.*, 2011, **47**, 7755–7757.
- N. J. Robinson and D. R. Winge, *Biochemistry*, 2010, **79**, 537–562.
- S. G. Kaler, *Nat. Rev. Neurol.*, 2011, **7**, 15–29.
- I. Bertini and A. Rosato, *Cell. Mol. Life Sci.*, 2008, **65**, 89–91.
- T. Finkel, M. Serrano and M. A. Blasco, *Nature*, 2007, **448**, 767–774.
- Q. Zou, X. Li, J. Zhang, J. Zhou, B. Sun and H. Tian, *Chem. Commun.*, 2012, **48**, 2095–2097.
- Z.-Q. Guo, W.-Q. Chen and X.-M. Duan, *Org. Lett.*, 2010, **12**, 2202–2205.
- S. Dalapati, S. Jana, M. A. Alam and N. Guchhait, *Sens. Actuators, B*, 2011, **160**, 1106–1111.
- N. Shao, G.-X. Pang, X.-R. Wang, R.-J. Wu and Y. Cheng, *Tetrahedron*, 2010, **66**, 7302–7308.
- W. T. Tak and S. C. Yoon, *Korean J. Nephrol.*, 2001, **20**, 863–871.
- W. Zhu, X. Huang, Z. Guo, X. Wu, H. Yu and H. Tian, *Chem. Commun.*, 2012, **48**, 1784–1786.
- Y. Kubo, T. Ishida, A. Kobayashi and T. D. James, *J. Mater. Chem.*, 2005, **15**, 2889–2895.
- Y. H. Lee, N. Park, Y. B. Park, Y. J. Hwang, C. Kang and J. S. Kim, *Chem. Commun.*, 2014, **50**, 3197–3200.
- J. P. Lorand and J. O. Edwards, *J. Org. Chem.*, 1959, **24**, 769–774.
- X. Zhang, L. Chi, S. Ji, Y. Wu, P. Song, K. Han, H. Guo, T. D. James and J. Zhao, *J. Am. Chem. Soc.*, 2009, **131**, 17452–17463.
- J. Zhao, T. M. Fyles and T. D. James, *Angew. Chem., Int. Ed.*, 2004, **43**, 3461–3464.
- Y.-J. Huang, W.-J. Ouyang, X. Wu, Z. Li, J. S. Fossey, T. D. James and Y.-B. Jiang, *J. Am. Chem. Soc.*, 2013, **135**, 1700–1703.
- K. M. K. Swamy, S.-K. Ko, S. K. Kwon, H. N. Lee, C. Mao, J.-M. Kim, K.-H. Lee, J. Kim, I. Shin and J. Yoon, *Chem. Commun.*, 2008, 5915–5917.
- S. K. Kim, K. Swamy, S.-Y. Chung, H. N. Kim, M. J. Kim, Y. Jeong and J. Yoon, *Tetrahedron Lett.*, 2010, **51**, 3286–3289.
- H. S. Jung, P. S. Kwon, J. W. Lee, J. I. Kim, C. S. Hong, J. W. Kim, S. Yan, J. Y. Lee, J. H. Lee, T. Joo and J. S. Kim, *J. Am. Chem. Soc.*, 2009, **131**, 2008–2012.
- Z. Chen, L. Wang, G. Zou, X. Cao, Y. Wu and P. Hu, *Spectrochim. Acta, Part A*, 2013, **114**, 323–329.
- S.-H. Li, F.-R. Chen, Y.-F. Zhou, J.-N. Wang, H. Zhang and J.-G. Xu, *Chem. Commun.*, 2009, 4179–4181.
- P. A. Waghorn, M. W. Jones, M. B. M. Theobald, R. L. Arrowsmith, S. I. Pascu, S. W. Botchway, S. Faulkner and J. R. Dilworth, *Chem. Sci.*, 2013, **4**, 1430–1441.
- R. L. Arrowsmith, P. A. Waghorn, M. W. Jones, A. Bauman, S. K. Brayshaw, Z. Y. Hu, G. Kociok-Kohn, T. L. Mindt, R. M. Tyrrel, S. W. Botchway, J. R. Dilworth and S. I. Pascu, *Dalton Trans.*, 2011, **40**(23), 6238–6252.
- B. McCranor, H. Zmacinski, H. H. Zeng, T. Hurst, A. Stoddard, C. A. Fierke, J. Lakowicz and R. B. Thompson, *Metallomics*, 2014, **6**, 1034–1042.
- A. Renfrew, N. S. Bryce and T. Hambley, *Chem. Sci.*, 2013, **4**, 3731–3739.
- J. R. Lakowicz, *Principles of fluorescence spectroscopy*, Springer, 4th edn, 2006.
- P. G. Bush, D. L. Wokosin and A. C. Hall, *Front. Biosci.*, 2007, **12**, 2646–2654.

